

# Magnetolectric coupling induced by exchange striction in frustrated Ising spin chain: Monte Carlo simulation

Xiaoyan Yao,<sup>1,a)</sup> Veng Cheong Lo,<sup>2</sup> and Jun-Ming Liu<sup>3</sup>

<sup>1</sup>Department of Physics, Southeast University, Nanjing 211189, China

<sup>2</sup>Department of Applied Physics, The Hong Kong Polytechnic University, Hong Kong, China

<sup>3</sup>Nanjing National Laboratory of Microstructures, Nanjing University, Nanjing 210093, China

(Received 21 November 2008; accepted 23 December 2008; published online 10 February 2009)

The fascinating magnetolectric behavior as observed in  $\text{Ca}_3\text{CoMnO}_6$  compound [Choi *et al.*, Phys. Rev. Lett. **100**, 047601 (2008)] is investigated by using Monte Carlo simulation based on a one-dimensional elastic Ising model. The macroscopic polarization results from the ionic displacements attributed to the exchange striction in an up-up-down-down ( $\uparrow\uparrow\downarrow\downarrow$ ) spin ordering. In this scenario, the microscopic structures of spin and ionic displacement are investigated at different temperatures under different external electric fields to illuminate in detail the microscopic mechanism of the strong coupling between the magnetism and the ferroelectricity. It is revealed that the change in spin configuration dependent on temperature induces the freezing and melting phenomena of the polarized domains and thus the complicated temperature-dependent ferroelectric behavior in the whole low temperature range, namely the decline of the macroscopic polarization and the broad peak of dielectric constant. On the other hand, an external electric field also has influence on the magnetic structure through affecting the ionic displacements. © 2009 American Institute of Physics. [DOI: 10.1063/1.3077261]

## I. INTRODUCTION

Multiferroicity, namely coexistence of two or more ferroic orders, has attracted considerable attention in recent years. Especially the magnetolectric (ME) compounds, which possess (anti)ferromagnetic (FM) and ferroelectric orders, have been extensively studied owing to the important application potentials and fundamental significance.<sup>1–4</sup> Currently the magnetism-driven ferroelectricity was discovered in many frustrated systems, which renewed the interest of investigation in this field.<sup>5–10</sup> The strong coupling between the electric polarization and the magnetic ordering in these compounds provides a possibility of simultaneously controlling magnetic and electric degrees of freedom. But the corresponding microscopic mechanism, which is very essential to achieve their potential applications, still remains a difficult task.

The investigation of the triangular spin-chain system has been an active direction of research for the past several decades. In this class of materials, the low dimensional structure and the geometrical frustration of spins induce the fascinating physical phenomena such as the multistep magnetization.<sup>11–14</sup> Recently the discovery of the multiferroicity in triangular spin-chain materials attracted more attention in this field.<sup>15,16</sup> Especially the experiment of Choi *et al.*<sup>17</sup> reported that the ferroelectricity driven by a collinear spin ordering was discovered in  $\text{Ca}_3\text{Co}_{2-x}\text{Mn}_x\text{O}_6$  ( $x \approx 0.96$  very near 1), which is very different from the noncollinear-magnetism-driven ferroelectricity that has been widely investigated.<sup>18–21</sup> This novel ferroelectric phenomenon has attracted a lot of attention. Wu *et al.*<sup>22</sup> and Zhang *et al.*<sup>23</sup>

investigated the microscopic structure of magnetism and ferroelectricity in  $\text{Ca}_3\text{CoMnO}_6$  by the density functional theory calculations and *ab initio* electronic structure calculations, respectively. They confirmed that the up-up-down-down spin ordering is the magnetic ground state of the system, and inequivalence of the Co–Mn distances accounts for the ferroelectricity.

$\text{Ca}_3\text{CoMnO}_6$  belongs to the family of triangular spin-chain compounds with the general formula  $A'_3ABO_6$  (where  $A'$  is Ca or Sr,  $A$  and  $B$  are transition metal elements). Such compounds consist of parallel one-dimensional (1D)  $ABO_6$  chains aligned along the hexagonal  $c$ -axis, separated by  $A'^{2+}$  ions, forming a triangular lattice in the  $ab$ -plane.<sup>24</sup> For  $\text{Ca}_3\text{CoMnO}_6$ , the magnetic chains consist of alternatively face-sharing  $\text{CoO}_6$  trigonal prisms with  $\text{Co}^{2+}$  ion and  $\text{MnO}_6$  octahedra with  $\text{Mn}^{4+}$  ion. The peculiar crystal field and the spin-orbit coupling induce a strong Ising-like anisotropy in this compound.<sup>22</sup> Based on these structure characters, this compound can be characterized by a 1D Ising model.<sup>17,25</sup>

Based on a 1D elastic Ising model, the present authors performed Monte Carlo (MC) simulation to investigate the collinear-magnetism-driven ferroelectricity observed in  $\text{Ca}_3\text{CoMnO}_6$ .<sup>26</sup> The preliminary results reproduced the temperature-dependent ferroelectric and magnetic behaviors of  $\text{Ca}_3\text{CoMnO}_6$  in the whole low temperature range, in qualitative agreement with the experimental data from Choi *et al.* In that work, it was confirmed that the macroscopic electric polarization is induced by the movements of magnetic ions, and the ionic displacements result from the exchange striction based on an up-up-down-down spin ordering. But the microscopic mechanism of the complex ferroelectric behavior dependent on temperature ( $T$ ) remains to be understood further. In this paper, we perform extensive simulation on

<sup>a)</sup>Electronic mail: yaoxiaoyan@gmail.com.

this 1D elastic Ising model to gain an insight into the microscopic scenario of this ME coupling. The microscopic structures of spins and ionic displacements are discussed in detail to comprehend the coupling between magnetism and ferroelectricity. It is indicated that the spin configuration changing with  $T$  induces the freezing and melting phenomena of polarization. Thus the complicated ferroelectric behavior dependent on  $T$  can be further comprehended in Ising chain magnet, which will be helpful for the future applications.

## II. MODEL AND SIMULATION

Aiming at the quasi-1D  $\text{Ca}_3\text{CoMnO}_6$ , Hamiltonian of this 1D Ising model can be written as

$$H = - \sum_{\langle i,j \rangle} J_{\text{FM}}(r_{ij}) S_i S_j - \sum_{[i,k]}^{Mn} J_{\text{AFMn}} S_i S_k - \sum_{[i,k]}^{\text{Co}} J_{\text{AFCo}} S_i S_k - hg \mu_B \sum_i S_i - E \sum_i q d_i + \frac{1}{2} k \sum_i d_i^2, \quad (1)$$

where  $S_i = \pm 1$  represents the  $i$ th spin of the chain. The first term on the right of Eq. (1) is the FM energy ( $J_{\text{FM}} > 0$ ), where  $\langle i, j \rangle$  denotes the summation over all the nearest-neighbor spin pairs. The second and the third terms are antiferromagnetic (AFM) energy with  $[i, j]$  signifying the summation over all the next-nearest-neighbor pairs, which is calculated for Mn and Co, respectively. The AFM coupling between each next-nearest-neighbor Mn–Mn pair is stronger than that for Co–Co ( $J_{\text{AFMn}} < J_{\text{AFCo}} < 0$ ).<sup>23</sup> The fourth term is the magnetic energy where  $h$  is the external magnetic field ( $h=0$  is always assumed except for the special clarification.),  $g$  is the Lande factor, and  $\mu_B$  is the Bohr magnetron. The fifth term denotes the electric energy where  $E$  is the electric field applied along the chain.  $q$  is the charge state of the moving ions, that is,  $q=2$  for  $\text{Co}^{2+}$ . The last term on the right of Eq. (1) is the elastic energy presented in the form of the harmonic potential, where  $k$  is the elastic constant with the value large enough to ensure the small values of the ionic displacements.

The exchange striction is considered for  $J_{\text{FM}}$ , so  $J_{\text{FM}}$  is dependent on the distance between the two nearest-neighbor spins. No matter what form of distance dependence for  $J_{\text{FM}}$  is, it can be expanded to the following linear approximation form:

$$J_{\text{FM}}(r_{i,i+1}) = J_{\text{FM}_0} \left( 1 + \eta \cdot \frac{r_{i,i+1} - r_0}{r_0} \right) = J_{\text{FM}_0} [1 + \eta(d_{i+1} - d_i)], \quad (2)$$

where  $J_{\text{FM}_0}$  is defined as the bare FM spin-spin interaction and  $\eta$  gives the strength of the coupling between the spin and the displacement.  $\eta < 0$  reflects that the interaction gets stronger as the spins get closer to each other.  $r_0$  is the original distance between two ions without the exchange striction;  $r_{i,i+1}$  is the distance between the  $i$ th ion and the  $(i+1)$ th ion under the exchange striction.  $d_i$  denotes the displacement of the  $i$ th ion normalized by  $r_0$  and it bears a positive value when this  $i$ th ion is approaching the  $(i+1)$ th one. According to Eq. (2), the change in  $J_{\text{FM}}$  is only related

TABLE I. System parameters chosen for the simulation.

Parameter	Value	Parameter	Value
$J_{\text{FM}_0}$	90	$\eta$	-8
$J_{\text{AFMn}}$	-65.7	$k$	34 000
$J_{\text{AFCo}}$	-7.3	$g$	2

to the distance between these two nearest-neighbor spins, therefore the relative movement of these two ions is the key for the exchange striction. For simplicity, it is assumed that only Co ions move, namely,  $d_i \neq 0$  for mobile Co ion, but  $d_i = 0$  for immobile Mn ion. For convenience,  $k_B$  is chosen to be unity, and the other parameters are scaled by the above assumption. Since the real values of these parameters are not available from experiments, they are chosen by the qualitative comparison between the simulated results and the experimental data, which had been discussed in Ref. 26. The values of these parameters for the simulation are shown in Table I.

The MC simulation is performed on a 1D Ising spin chain (of the system size  $L=4000$ ) with periodic boundary condition. The spin and the displacement are updated according to the Metropolis algorithm, respectively. Similar to the measurement process in the experiment,<sup>17</sup> the system is initially polarized by a large electric field of  $E_0=160$  at low temperature ( $T=1$ ). After  $E_0$  has been removed, the ferroelectric polarization ( $P$ ) and dc magnetic susceptibility ( $\chi = M/h$ ) are calculated with  $T$  increasing under a small electric field  $E$ . Here  $\chi$  is evaluated upon a small magnetic field  $h=0.15$ . The electric susceptibility  $\chi_e$  is calculated based on the statistic fluctuation, namely,<sup>27</sup>

$$\chi_e = \frac{\langle P^2 \rangle - \langle P \rangle^2}{T}. \quad (3)$$

Then the relative dielectric constant ( $\varepsilon$ ) is calculated by

$$\varepsilon = \chi_e + 1. \quad (4)$$

For every  $T$ , the initial 300 000 MC steps (MCSs) are discarded for equilibration. Moreover, then 10 000 data are collected at every five MCS to get an average result. The final results are obtained by averaging more than ten independent data sets obtained by selecting different seeds for random number generation.

In order to explore the magnetism-driven ferroelectricity at a microscopic level, we focus on the microscopic domain's size distribution scheme. In detail two structure parameters are proposed: (1) spin domain number (SDN), which is dependent on the size of spin domain ( $n_s$ ). The spin domain in this 1D case is defined as the spin area composed of the neighboring spins with the same orientation. For example, if  $S_1 = -S_2$ ,  $S_2 = S_3 = S_4 = S_5$ ,  $S_6 = -S_5$ , then  $S_2 \sim S_5$  constitute a spin domain with  $n_s = 4$ . Here SDN( $n_s$ ) is defined as the amount of the spin domains including  $n_s$  spins. The distribution of SDN on  $n_s$  shows the main character of the spin configuration. Moreover, the evolution of SDN( $n_s$ ) with  $T$  presents the useful information on the  $T$ -dependence of spin structure. (2) Displacement domain number (DDN). It is a function of the displacement domain's size ( $n_d$ ). Thus

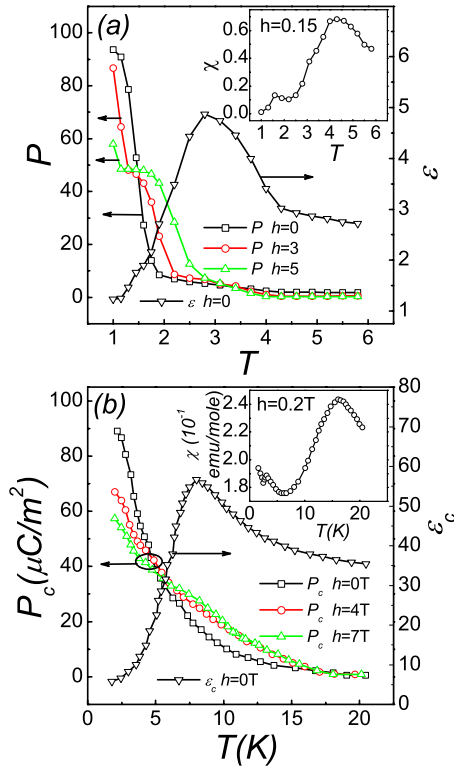


FIG. 1. (Color online) (a) Polarization  $P$  against temperature  $T$  under  $h=0, 3,$  and  $5$  when  $E=1$ . Dielectric constant  $\epsilon$  as a function of  $T$  with  $h=0$  and  $E=1$ . The insert gives the temperature dependence of dc magnetic susceptibility  $\chi$  under a small magnetic field  $h=0.15$  at  $E=1$ . (b) The corresponding experimental results of  $P_c$ ,  $\epsilon_c$ , and  $\chi$  in  $\text{Ca}_3\text{CoMnO}_6$  are reproduced from Ref. 17 to draw a qualitative comparison.

DDN( $n_d$ ) is defined as the amount of the displacement domains with  $n_d$  mobile ions. Here positive and negative displacement (ND) domains are counted, respectively. The positive displacement domain (PD domain) is defined as the ion area composed of the neighboring mobile ions with PDs larger than 0.01, while the neighboring mobile ions with NDs smaller than  $-0.01$  form the ND domain. For example, if  $d_1 < 0.01$ ,  $d_2, d_3, d_4$  and  $d_5 > 0.01$ ,  $d_6 < 0.01$ , then  $d_2 \sim d_5$  constitute a PD domain with  $n_d=4$ . The distribution of DDN on  $n_d$  presents more information on the microscopic character of the ferroelectric polarization in different conditions.

### III. RESULTS AND DISCUSSION

As replotted in Fig. 1(a), the simulation results show the complicated ferroelectric behavior in the whole low temperature range, consisting with the experimental results of  $\text{Ca}_3\text{CoMnO}_6$  [Fig. 1(b)] qualitatively.<sup>17,26</sup> A macroscopic  $P$  emerges at low temperature after the system has been polarized by a high electric field. With  $T$  increasing,  $P$  decreases rapidly at first. Then the decline of  $P$  becomes slow, and  $\epsilon$  reveals a broad peak in this temperature range. When  $T$  is raised further,  $\chi(T)$  curve presents a broad peak under a weak magnetic field  $h=0.15$  as illustrated in the inset of Fig. 1(a). At the same time,  $P$  fades away and the curve of  $\epsilon$  against  $T$  starts a linear paraelectric behavior above that temperature. All these phenomena imply a transition to paramagnetic and paraelectric phases taking place at about  $T_p \approx 4.3$ . The application of magnetic field has a complicated influ-

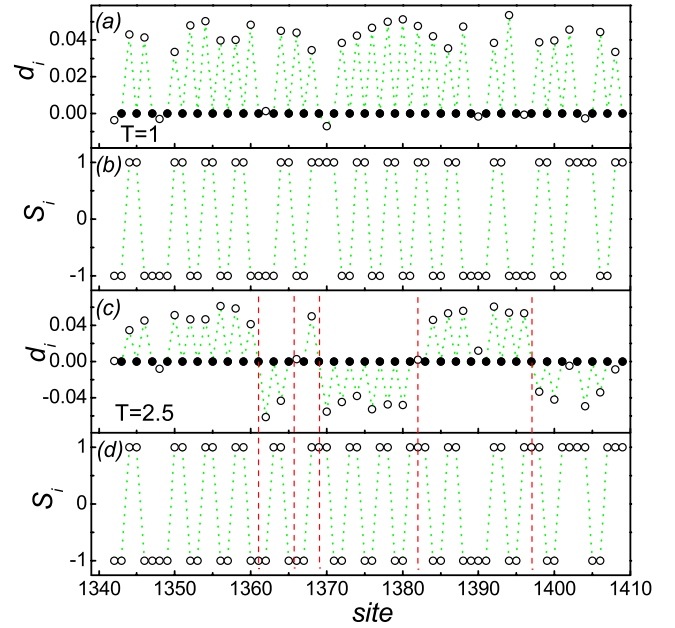


FIG. 2. (Color online) (a) Partial snapshot for the displacements of ions in a chain and (b) the corresponding snapshot of spins at  $T=1$  and  $E=1$ . (c) Partial snapshot for the ionic displacements and (d) the corresponding snapshot of spins at  $T=2.5$  and  $E=1$ . Here the hollow circles denote the mobile ions moving along the chain, and the solid ones represent the immobile ions. The red dashed lines mark the switch points of displacement direction and the corresponding odd-spin domains.

ence on the ferroelectric behavior below  $T_p$ , namely,  $h$  suppresses  $P$  at first and then enhances  $P$  with  $T$  increasing. Additionally, as  $h$  is raised, this influence becomes more obvious.

The complicated ferroelectric behavior can be understood by the microscopic scenario of ionic displacements. The spin frustration, resulting from the competition between the nearest-neighbor FM and next-nearest-neighbor AFM interactions, induces an up-up-down-down spin ordering. Then the exchange striction makes the ions move along the chain in this up-up-down-down spin state. The high polarizing electric field imposes a dominant direction for ionic displacements, and thus the system demonstrates a macroscopic  $P$ . As presented in Figs. 2(a) and 2(b), many ferroelectric domains clamped with the short-ranged up-up-down-down ordering exist at  $T=1$ . These displacement domains keep to the direction of the polarizing field even after the polarizing field has been removed, namely they are frozen. But when  $T$  increases, these frozen domains gradually melt and the displacements of ions cannot keep to the polarized direction anymore. As shown in Fig. 2(c), many displacement domains with the opposite directions exist at  $T=2.5$ . The counteraction between these domains with two opposite directions leads to the sharp decrease in macroscopic  $P$ .

The freezing and melting of these displacement domains are attributed to some particular spin structures. When  $P$  decreases with  $T$  increasing, the character of spin configuration changes a lot. As illustrated in Fig. 4(a), SDN( $n_s$ ) curve at  $T=1$  presents a special feature, that is, only spin domains with even spins (even-spin domain) exist, and there are almost no domains including odd spins (odd-spin domain). So the  $n_s$  distribution of SDN at  $T=1$  shows a hackly shape.

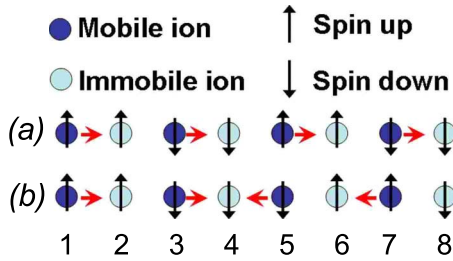


FIG. 3. (Color online) (a) The sketch of Ising chain with the up-up-down-down spin order and alternating ionic order. (b) The sketch of ionic chain with an odd-spin domain. The red arrow presents the direction of displacement for the mobile ion.

Similar to the frustrated 1D Ising chain without exchange striction,<sup>28</sup> as  $T$  is raised the odd-spin domains appear and increase, at the same time the amount of even-spin domains decreases. When  $T=2.5$ ,  $SDN(n_s)$  curve becomes smooth. Therefore, it is worthwhile to note that the odd-spin domain and even-spin domain play different roles for the ferroelectric property of the system, as illustrated in Fig. 3. For sketch (a) there are only even-spin domains. All the mobile ions move to the right because they and their right neighbors have the same spin orientation, and the exchange striction, which shrinks the bond lengths between the parallel spins and stretches those between the antiparallel spins, makes them move right. The ion with the opposite displacement will enhance the energy of exchange striction, and consequently it is suppressed greatly. As shown in Figs. 2(a) and 2(b), the chain at  $T=1$  is composed of the even-spin domains, and consequently most ionic displacements take the same direction which is consistent with the direction of the polarizing field to reserve the low level of the energy. But for sketch (b) in Fig. 3, an odd-spin domain breaks the uniform ionic displacements. The fifth ion, which is in an odd-spin domain, has to switch its displacement direction because its spin orientation is parallel to its left neighbor. Beginning from the fifth ion, the residual mobile ions have the same spin orientation to their left neighboring ions, and then have to move to the left. Therefore the odd-spin domain gives the chance to the corresponding ionic displacement to flip to the opposite direction. Then the domains with the opposite direction appear. As presented in Figs. 2(c) and 2(d) at  $T=2.5$ , everywhere an odd-spin domain appears, the ionic displacement changes its direction to reduce the energy of the exchange striction. The existence of many odd-spin domains induces a lot of short-ranged displacement domains with opposite directions. Thus, it is indicated that the even-spin domain is very important for the ionic displacements to reserve the polarized direction. On the contrary, the odd-spin domain helps the emergence of the opposite displacement domains. The spin structure has great influence on the size distribution of displacement domains, as demonstrated in the inset of Fig. 4(a). At  $T=1$ ,  $DDN(n_d)$  curve for PD domain is much higher than that for ND domain, namely the PD domains are far more than ND domains, and there are only few ND domains. Therefore macroscopic  $P$  has a high value. In other words,  $P$  is frozen in the polarized direction due to the even-spin domains. When  $T$  is raised, the odd-spin domains appear and then increase, which produces more and more ND domains.

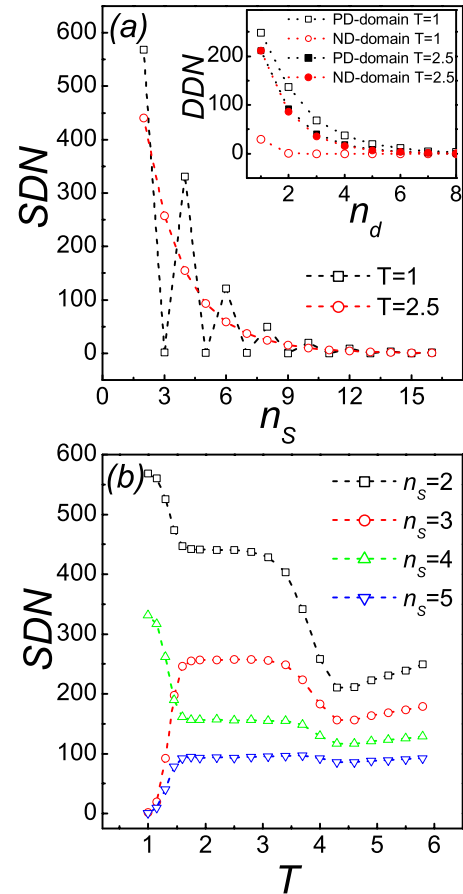


FIG. 4. (Color online) At  $E=1$ , (a)  $SDN(n_s)$  curves at  $T=1$  and 2.5. The inset presents  $DDN(n_d)$  curves for PD domain and ND domain at  $T=1$  and 2.5, respectively. (b)  $SDN$  as functions of  $T$  for  $n_s=2, 3, 4$ , and 5.

When  $T=2.5$ , the amount of ND domains is just a little lower than that of PD domains, as shown in the inset of Fig. 4(a). Therefore counteraction between the PDs and negative ones produces a low value of  $P$ . In other words, the polarized ferroelectric domains melt due to the emergence of the odd-spin domains.

In order to further understand the  $T$ -dependence of spin structure,  $SDNs$  as a function of  $T$  for the spin domains with 2, 3, 4, and 5 spins ( $n_s=2, 3, 4$ , and 5) in the whole low  $T$  range are plotted in Fig. 4(b). At  $T=1$ , consisting with Fig. 4(a), the amounts of odd-spin domains are about zero, and those of even-spin domains show a high value. When  $T$  is raised, the even-spin domains decrease, but the odd-spin domains increase to a relatively high quantity. Then the amounts of different spin domains reserve their values until the anomaly emerging at about  $T_p=4.3$ . Corresponding to the transition to the paramagnetic state, the spin domains are reduced obviously at this temperature. The plateau behavior of spin domains with plenty of odd-spin domains brings many active displacement domains into the system. In this temperature range, these displacement domains are sensitive to the external electric field. As illustrated in Fig. 5(a), a small change in  $E$  has an obvious influence on  $P$  in this temperature range, but hardly affects  $P$  at other temperatures. When  $E$  is enhanced,  $P$  presents a higher value. Therefore,  $\epsilon$  demonstrates a broad peak in this temperature range. More-



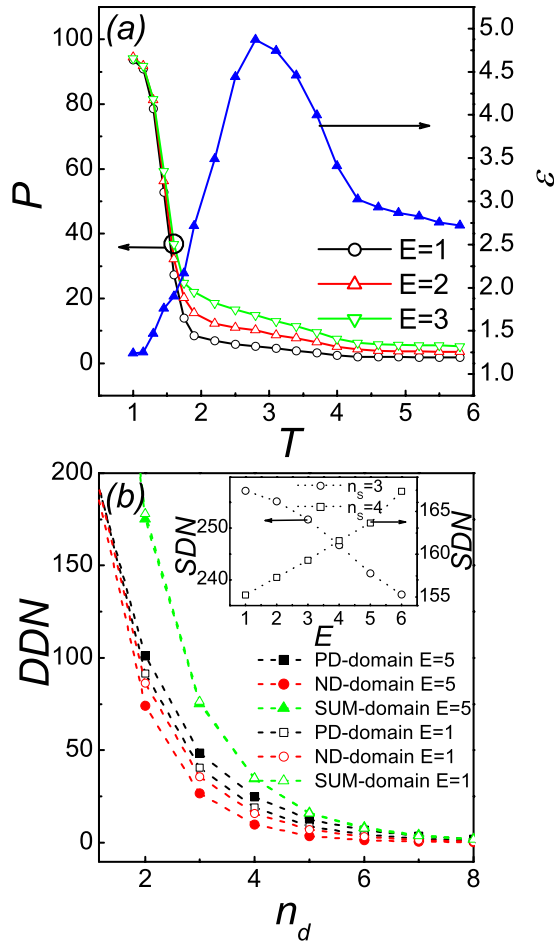


FIG. 5. (Color online) (a) Dielectric constant  $\epsilon$  at  $E=1$  and polarization  $P$  under  $E=1, 2$ , and  $3$  against temperature  $T$ . (b) DDN( $n_d$ ) curves for PD domain, ND domain, and sum domain at  $T=2.5$  when  $E=1$  and  $5$ , respectively. The inset presents SDN as functions of  $E$  with  $n_s=3$  and  $4$  at  $T=2.5$ .

over, the effect that  $E$  takes on the microscopic structure of ionic displacements is shown in Fig. 5(b). As  $T=2.5$ , it is seen that at  $E=1$  the amount of PD domains is close to that of ND domains. But when  $E=5$ , the amount of PD domains is higher than that of ND domains obviously. The electric field enhances the PD domains with the displacements along the direction of  $E$ , but suppresses ND domains with the opposite direction. It is interesting that for a certain  $n_d$  the total amounts of the displacement domains (sum domains, i.e., the sum of PD domains and ND domains) upon  $E=1$  and  $E=5$  are almost equal. It means that a small electric field has nearly no influence on the size distribution of sum domains. It just changes the direction of displacement domains and aligns some opposite domains along the orientation of  $E$ . Consequently  $P$  is enhanced with  $E$  increasing. The external electrical field also affects the spin structure through the ionic displacements. As mentioned above, a direction switch of ionic displacement corresponds to an odd-spin domain. With ND domains decreasing and thus the switch points of displacement direction decreasing, the odd-spin domains are suppressed gradually as  $E$  increases. At the same time, the even-spin domains are enhanced, which is illustrated in the insert of Fig. 5(b).

## IV. CONCLUSION

In summary, the ME coupling induced by the exchange striction in a frustrated Ising spin chain is investigated by using MC simulation to comprehend the collinear-magnetism-driven ferroelectricity observed in  $\text{Ca}_3\text{CoMnO}_6$ . The complicated ferroelectric behavior and its magnetic mechanism are discussed extensively. Moreover, the microscopic structure characters of spin configuration and ionic displacement are presented at different  $T$  and different  $E$ . It is indicated that the spin domain including odd or even spins plays very different roles in the exchange striction of the collinear magnetic system, and therefore induces the freezing or melting phenomena of the polarized domains. The strong coupling between microscopic spin and ionic displacement results in the fascinating behaviors of  $P$  and  $\epsilon$  against  $T$ . Although the real material is far more complicated than the present model, we believe that the present work would help to understand the coupling between magnetic and electric degrees of freedom in the frustrated magnet, and shed light for the potential applications.

## ACKNOWLEDGMENTS

This work is supported by the research grants from the National Natural Science Foundation of China (Grant No. 10747115, 50832002) and the National Key Projects for Basic Researches of China (2006CB623303).

- <sup>1</sup>R. Ramesh and N. A. Spaldin, *Nature Mater.* **6**, 21 (2007).
- <sup>2</sup>T. Zhao, A. Scholl, F. Zavalche, K. Lee, M. Barry, A. Doran, M. P. Cruz, Y. H. Chu, C. Ederer, N. A. Spaldin, R. R. Das, D. M. Kim, S. H. Baek, C. B. Eom, and R. Ramesh, *Nature Mater.* **5**, 823 (2006).
- <sup>3</sup>N. A. Spaldin and M. Fiebig, *Science* **309**, 391 (2005).
- <sup>4</sup>G. L. Yuan, S. W. Or, and H. L. W. Chan, *J. Appl. Phys.* **101**, 064101 (2007).
- <sup>5</sup>T. Kimura, T. Goto, H. Shintani, K. Ishizaka, T. Arima, and Y. Tokura, *Nature (London)* **426**, 55 (2003).
- <sup>6</sup>T. Kimura, G. Lawes, and A. P. Ramirez, *Phys. Rev. Lett.* **94**, 137201 (2005).
- <sup>7</sup>G. Lawes, A. B. Harris, T. Kimura, N. Rogado, R. J. Cava, A. Aharony, O. Entin-Wohlman, T. Yildirim, M. Kenzelmann, C. Broholm, and A. P. Ramirez, *Phys. Rev. Lett.* **95**, 087205 (2005).
- <sup>8</sup>K. Taniguchi, N. Abe, T. Takenobu, Y. Iwasa, and T. Arima, *Phys. Rev. Lett.* **97**, 097203 (2006).
- <sup>9</sup>S. Park, Y. J. Choi, C. L. Zhang, and S.-W. Cheong, *Phys. Rev. Lett.* **98**, 057601 (2007).
- <sup>10</sup>J. M. Wesselinowa and S. Kovachev, *J. Appl. Phys.* **102**, 043911 (2007).
- <sup>11</sup>X. Yao, S. Dong, H. Yu, and J. Liu, *Phys. Rev. B* **74**, 134421 (2006).
- <sup>12</sup>V. Hardy, M. R. Lees, O. A. Petrenko, D. M. Paul, D. Flahaut, S. Hébert, and A. Maignan, *Phys. Rev. B* **70**, 064424 (2004).
- <sup>13</sup>X. Yao, S. Dong, K. Xia, P. Li, and J.-M. Liu, *Phys. Rev. B* **76**, 024435 (2007).
- <sup>14</sup>X. Yao, S. Dong, and J.-M. Liu, *Phys. Rev. B* **73**, 212415 (2006).
- <sup>15</sup>N. Bellido, C. Simon, and A. Maignan, *Phys. Rev. B* **77**, 054430 (2008).
- <sup>16</sup>P. L. Li, X. Yao, K. F. Wang, C. L. Lu, F. Gao, and J.-M. Liu, *J. Appl. Phys.* **104**, 054111 (2008).
- <sup>17</sup>Y. J. Choi, H. T. Yi, S. Lee, Q. Huang, V. Kiryukhin, and S.-W. Cheong, *Phys. Rev. Lett.* **100**, 047601 (2008).
- <sup>18</sup>H. Katsura, N. Nagaosa, and A. V. Balatsky, *Phys. Rev. Lett.* **95**, 057205 (2005).
- <sup>19</sup>I. A. Sergienko and E. Dagotto, *Phys. Rev. B* **73**, 094434 (2006).
- <sup>20</sup>Q. C. Li, S. Dong, and J.-M. Liu, *Phys. Rev. B* **77**, 054442 (2008).
- <sup>21</sup>S.-W. Cheong and M. Mostovoy, *Nature Mater.* **6**, 13 (2007).
- <sup>22</sup>H. Wu, T. Burnus, Z. Hu, C. Martin, A. Maignan, J. C. Cezar, A. Tanaka, N. B. Brookes, D. I. Khomskii, and L. H. Tjeng, *Phys. Rev. Lett.* **102**(2), 026404 (2009).
- <sup>23</sup>Y. Zhang, H. J. Xiang, and M.-H. Whangbo, e-print arXiv:0809.1234.

- <sup>24</sup>H. Fjellvag, E. Gulbrandsen, S. Aasland, A. Olsen, and B. C. Hauback, *J. Solid State Chem.* **124**, 190 (1996).
- <sup>25</sup>V. G. Zubkov, G. V. Bazuev, A. P. Tyutyunnik, and I. F. Berger, *J. Solid State Chem.* **160**, 293 (2001).
- <sup>26</sup>X. Yao and V. C. Lo, *J. Appl. Phys.* **104**, 083919 (2008).
- <sup>27</sup>V. Privman, *Finite Size Scaling and Numerical Simulation of Statistical System* (World Scientific, Singapore, 1990).
- <sup>28</sup>M. E. Fisher and W. Selke, *Phys. Rev. Lett.* **44**, 1502 (1980).